ELSEVIER

Thermochimica Acta 376 (2001) 155–162

thermochimica acta

www.elsevier.com/locate/tca

Thermal analysis of large pore microporous zincophosphates

Luz Arcelia García-Serrano[a,1], Fernando Rey[b], Joaquín Pérez-Pariente[a], Enrique Sastre[a,*]

[a]*Instituto de Catálisis y Petroleoquímica, C.S.I.C., Campus Cantoblanco, 28049 Madrid, Spain*
[b]*Instituto de Tecnología Química, U.P.V.-C.S.I.C., Avd. de los Naranjos s/n, 46022 Valencia, Spain*

Received 23 April 2001; accepted 8 May 2001

Abstract

Samples of tridimensional microporous zinc phosphates with fully connected framework with faujasite (FAU) and chiral zincophosphate (CZP) structures have been prepared and characterized by thermal analyses comprising TGA, TGA–MS and in situ thermal XRD. They have been also characterized by ICP and ^{13}C MAS NMR.

Analyses of the ZnPO–FAU demonstrate that the tetramethylammonium (TMA^+) cations are incorporated preferentially in the β-cages and that this material is stable up to 673 K. The crystallinity of the sample only decreases when the TMA^+ cations located in the β-cages are eliminated (above ∼723 K).

In the case on ZnPO–CZP the thermal removal of the water more strongly held by the structure produces a marked decrease of crystallinity at ∼523 K © 2001 Elsevier Science B.V. All rights reserved.

Keywords: Crystalline microporous zincophosphates; Thermal stability; In situ thermal XRD

1. Introduction

During the last few years, an increasing number of papers have described the synthesis of a variety of novel open-framework zincophosphates [1,2]. It has also been described the preparation of a large number of materials in the zinc–phosphorous–oxygen system with layered and non-porous structures [3–7]. In some cases the materials synthesized have the structure of analogous well known aluminosilicate frameworks such as faujasite (FAU) [8–11] or sodalite [8,12]. In other cases, new large pore microporous materials with no counterpart in the field of zeolites have been described, such as the structure known as chiral zincophosphate (CZP) [13,14] code assigned by the International Zeolite Association (IZA) [15].

Such as in the case of zeolites, microporous zincophosphates have potential applications as adsorbents and catalysts. Specially, in this latter field large pore materials as those with CZP and FAU structures have demonstrated interesting properties in base catalyzed reactions such as the Knoevenagel condensation of benzaldehyde with activated methylenic compounds [16,17] or the Michael addition of nitroethane to olefin with different steric demand, acroleine and 2-phenylacroleine [17]. The structures of these two zincophosphates are defined by a 12 member ring (12 MR) channel system, tridirectional in the case of the FAU and along the c axis in the CZP structure. In the later case, the channels are accessible through puckered 12-ring openings of 3.7 Å × 7.5 Å and in the case of the

* Corresponding author. Fax: +34-91-585-4760.
E-mail address: esastre@icp.csic.es (E. Sastre).
[1] Present address: Instituto Mexicano del Petróleo, México D.F., Mexico.

0040-6031/01/$ – see front matter © 2001 Elsevier Science B.V. All rights reserved.
PII: S0040-6031(01)00564-0

FAU, the channels present a pore opening of 7.4 Å with large cages of 12 Å in the crossings.

In order to improve their application as catalysts, it could be very important to study the thermal properties and stability of these materials. Very few papers have been published dealing with detailed studies of the thermal stability of the different microporous zincophosphates. Rajic et al. [18] studied the influence of Co(II) incorporation in two different porous zincophosphates on their thermal properties, one of them with a structure similar to the sodalite aluminosilicate and the other described as a hexagonal phase which, according to the X-ray diffraction pattern presented in the paper, corresponds to the CZP structure [15].

The aim of this paper is to perform a detailed study of the thermal properties and specially the thermal stability of two large pore microporous zincophosphates having faujasite (ZnPO–FAU) and chiral (ZnPO–CZP) structures.

2. Experimental

2.1. Synthesis

Synthesis gels with the molar composition: wP_2O_5:ZnO:xNa_2O:$yTMA_2O$:zH_2O were prepared from phosphoric acid (Riedel de Haen, 85 wt.%), sodium hydroxide (Prolabo, 99.7 wt.%), zinc nitrate (Aldrich, >99 wt.%) and tetramethylammonium hydroxide pentahydrate (Aldrich, >99 wt.%). The specific gel composition and synthesis conditions resulting in the different pure crystalline phases are given in Table 1.

The general synthesis procedure can be conveniently illustrated by the following typical example, which best yield nearly pure crystals of ZnPO–FAU.

A solution of 0.57 g of NaOH in 28 g of water (35% of the total water) is prepared in a polypropylene bottle kept in an ice bath cooled to 277 K. Then 10.91 g of TMAOH and 3.31 g of H_3PO_4 are very slowly added to this solution. The reaction is exothermic, and once the solution is again at 277 K, 6.39 g of zinc nitrate dissolved in the remaining water (52 g) previously cooled to 277 K is added drop by drop under stirring. Then, the formed gel is poured into polypropylene bottles which are kept in a refrigerated room at 277 K for selected periods of time. The samples were filtered and washed with deionized water and dried at 313 K.

2.2. Characterization

XRD measurements were carried out on a SEIFERT XRD 3000P diffractometer, using the Cu Kα radiation. XRD experiments related with the thermal stability of the samples were performed under vacuum on a Philips PW 1710 diffractometer equipped with a high temperature chamber. Chemical analysis of Zn, Na and P were performed by inductive coupled plasma emission spectroscopy (Perkin-Elmer OPTIMA 3300 DV), whereas C, H and N were determined in a Perkin-Elmer 2400 analyzer.

Thermal analyses were done on a Perkin-Elmer TGA 7 instrument (∼5 mg of sample, helium = 50 $cm^3\ min^{-1}$, heating rate = 10 K min^{-1}).

On-line thermogravimetric–mass spectrometry analyses (TG–MS) of the gases evolved from the sample were carried out on the Perkin-Elmer TGA 7 thermobalance coupled to a Fisons MD-800 quadrupolar mass spectrometer through a transfer line heated at 423 K. The TGA was operated from 303 to 1173 K at 20 K min^{-1} under a continuous flow of He (100 $cm^3\ min^{-1}$). A Perkin-Elmer transfer line, specially designed to avoid mass discrimination and

Table 1
Chemical composition of the synthesis gel and crystallization parameters for each structure[a]

Sample	Crystallization time (h)	Gelification temperature (K)	Molar composition of the gel (ZnO = 1)			
			P_2O_5 (w)	Na_2O (x)	TMA_2O (y)	H_2O (z)
ZnPO–FAU	5	277	0.7	0.30	1.4	228
ZnPO–CZP	5	277	0.9	0.54	2.2	347
Hopeite	8	298	0.7	0.30	1.4	228

[a] Crystallization temperature T = 277 K.

connected to a vacuum pump in order to optimize the amount of gas sample transferred from the TG to the MS, carries on the evolved gas to the mass spectrometer. The ionization of the sample was done by electronic impact, 70 eV, and a mass analysis is performed each 2 s recording mass fragments between 2 and 350 amu.

Solid-state ^{13}C NMR were recorded under magic-angle spinning (MAS) at ambient temperature on a Varian VXR-400S WB spectrometer at 100.6 MHz, using a CP/MAS Varian probe with zircona rotors (5 mm in diameter). The ^{13}C NMR spectrum was recorded using $\pi/4$ pulses of 3 μs, with high power decoupling for protons, and a repetition time of 15 s, with the sample spinning at 5.5 kHz.

3. Results and discussion

3.1. Synthesis and characterization of crystalline samples

In the synthesis system described early, in general three phases can be obtained: faujasite (FAU), the hexagonal chiral phase (CZP) and hopeite, a dense phase with chemical composition $Zn_3(PO_4)_2{\cdot}4H_2O$ [19]. The specific synthesis conditions for each structure are given in Table 1.

Chemical compositions of the samples of hopeite, ZnPO–CZP and ZnPO–FAU are given in Table 2. The P/Zn ratios fit reasonably well the expected stoichiometries, although a defect of phosphorous is detected in the hexagonal phase CZP (theoretically P/Zn = 1). The Na content in FAU is somewhat lower than expected, and it is absent in hopeite. On the other hand, the CZP phase contains very small amount of organic material, which is absent in hopeite. From the chemical analysis of FAU, it can be deduced that there are ∼8 TMA^+ cations per unit cell. Although this figure matches the number of sodalite cages per unit cell, it does not necessarily imply that all of them are actually occupied by tetramethylammoniun cations.

3.2. Thermogravimetric–mass spectrometry analyses

The mass spectrometry coupled with the thermogravimetric analysis can help in determining the location of the TMA^+ cations present in the structure. The results are plotted in Fig. 1 for sample ZnPO–FAU. Three thermal events centered at ∼403, 573 and 743 K are observed. The first one can be assigned to the desorption of water, whereas the two other are essentially due to the elimination of organic material, as can be seen by monitoring the masses 42 and 58 amu, characteristic of the trimethylamine, the principal decomposition product of the TMA^+ cations, which are the most intense lines of the mass spectrum of the evolved gas. The high temperature weight loss is by far more intense than the one at ∼573 K. These results can be compared with the ones previously reported by Saldarriaga et al. [20] on TMA–FAU and SAPO-37. These authors show that the weight loss of TMA–FAU at ∼573 K corresponds to TMA^+ in the supercage, whereas the one at higher temperature is from TMA^+ residing in the β-cages. Furthermore, it is quite reasonable to found that the TMA^+ in the small β-cage decompose at higher temperature than the one located in the more open supercage. This assignation is also supported by the fact that the total weight loss in air between 533 and 823 K matches the organic content determined by chemical analysis. Indeed, the ^{13}C

Table 2
Chemical and thermal analysis of the samples

Sample	Chemical analysis						TGA[a]
	mol/100 g			wt.%			
	P	Zn	Na	C	N	H	
ZnPO–FAU	0.47	0.49	0.32	1.94	0.60	1.65	17.5
Hopeite	0.45	0.61	0	0.02	0.06	1.06	16.0
ZnPO–CZP	0.38	0.50	0.52	0.20	0.12	1.08	10.5

[a] Total weight loss between 298 and 1123 K.

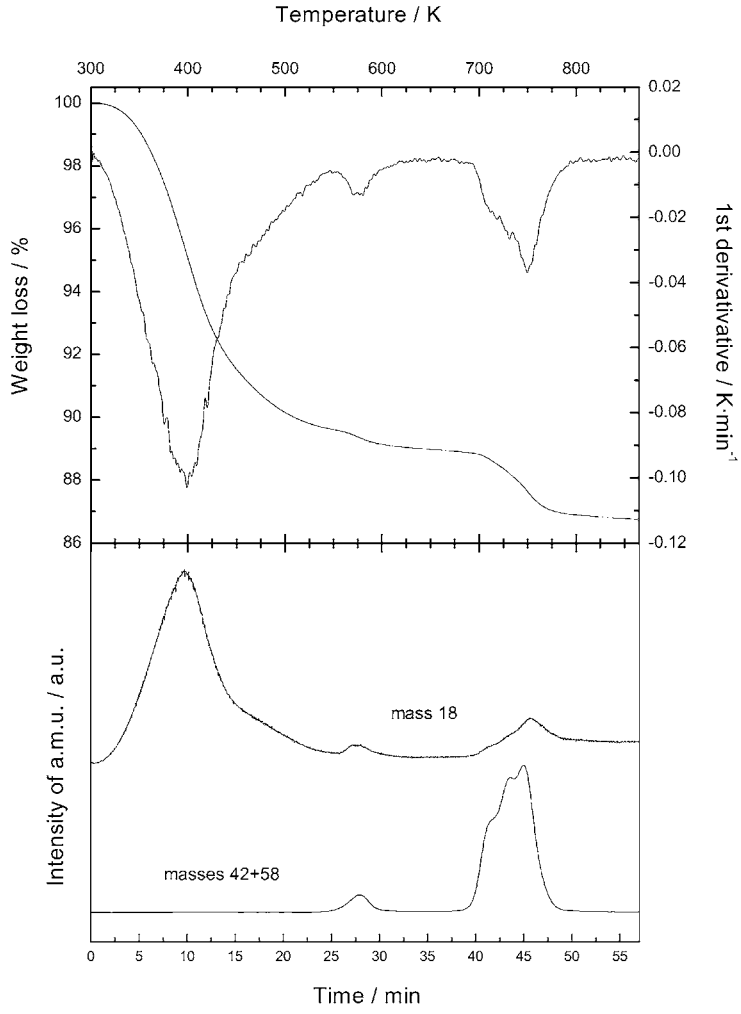

Fig. 1. TGA–MS of sample ZnPO–FAU. MS curves representative of water (MS = 18) and trimethylamine (MS = 42 + 58) are plotted.

MAS NMR spectra of this sample (Fig. 2) consists of two resonances at 56.0 and 58.3 ppm attributed to TMA^+ cations located in the supercage and sodalite units, respectively [21]. The relative intensity of both peaks indicates that approximately one-forth of the TMA^+ are in the supercages, which corresponds closely to the relative populations of those sites as determined by TGA. This result confirms the hypothesis advanced previously by Harrison et al. [9] on the location of TMA^+ into the ZnPO–FAU structure, although their material have 12 TMA^+ per unit cell. This discrepancy could be eventually attributed to the differences in the synthesis conditions used to prepare both samples.

3.3. Themogravimetric analyses

Fig. 3 shows the TG results for hopeite. Two well defined stages of nearly equivalent weight losses are observed centered at ~383 and 610 K, respectively. This two losses should correspond to desorption of water, as no organic species are present in the sample. Indeed, a total weight loss of 16.0 wt.% is obtained, which compared quite well with the predicted value of 15.7 wt.% from the stoichiometry of hopeite $Zn_3(PO_4)_2{\cdot}4H_2O$. The four water molecules of this compound are located in the first coordination shell of octahedral $ZnO_2(H_2O)_4$ entities [19]. Then, the

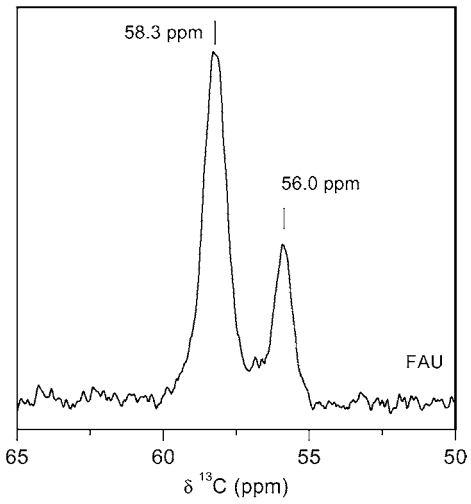

Fig. 2. ^{13}C MAS NMR spectrum of sample ZnPO–FAU.

desorption of half of the water molecules which takes place at 383 K causes the transition from octahedrally to tetrahedrally coordinated Zn^{2+} cations. The remaining water is more strongly retained by the tetrahedral Zn^{2+}, and desorbs completely at $T > 573$ K.

The thermogravimetric analysis of the CZP phase is shown in Fig. 4. It can be observed there a first weight loss at $T < 333$ K, caused by the removal of physically adsorbed water. This is followed by a smooth weight loss up to ~523 K, and finally a very sharp peak (detected in the derivative plot) centered at 573 K is observed, which corresponds to a weight loss of about 40% of the previous one. The total weight loss from 333 to 873 K is 9.4 wt.%, which closely approaches the 8.4 wt.% corresponding to the stoichiometry of CZP, $NaZnPO_4 \cdot H_2O$. The TG/DTA pattern of this hexagonal phase has already been reported [14,18] and agrees with the one described here. Nevertheless, the weight losses have not yet been assigned. Indeed, it is rather surprising to found water desorbed at temperature as high as 573 K, taking into account that the reported structure of this material is formed by corner sharing tetrahedral [ZnO_4] and [PO_4] units, where the water is solvating the Na^+ cations located in the cavities [3,14]. Detailed TG analysis of sodium zinc phosphates which could be used as references for TG step assignation are scarcely reported in the literature. In one of those examples, Harrison et al. [22] attributed a weight loss of the material $Na_2ZnPO_4OH \cdot 7H_2O$ in the range 323–403 K to the desorption of the water coordinated to the Na^+ cations, whereas the P–OH hydroxyl groups are lost at higher temperature. In the compound $Na_3Zn_4O(PO_4)_3 \cdot 6H_2O$ the solvation water of the Na^+ cations is lost up to 433 K [23]. On the other hand, in the structure $Zn_4(PO_4)_2(HPO_4)_2 \cdot 3H_2O$. The compound $H_2N_2C_6H_{12}$ with an interrupted framework formed

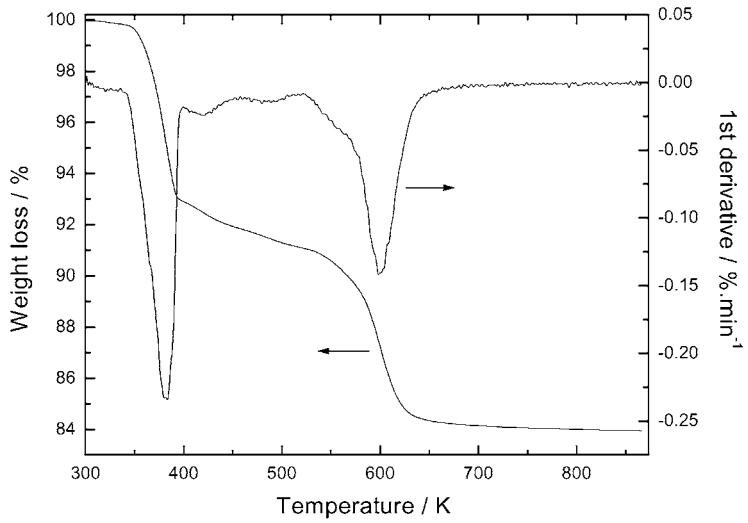

Fig. 3. TGA and DTG of hopeite.

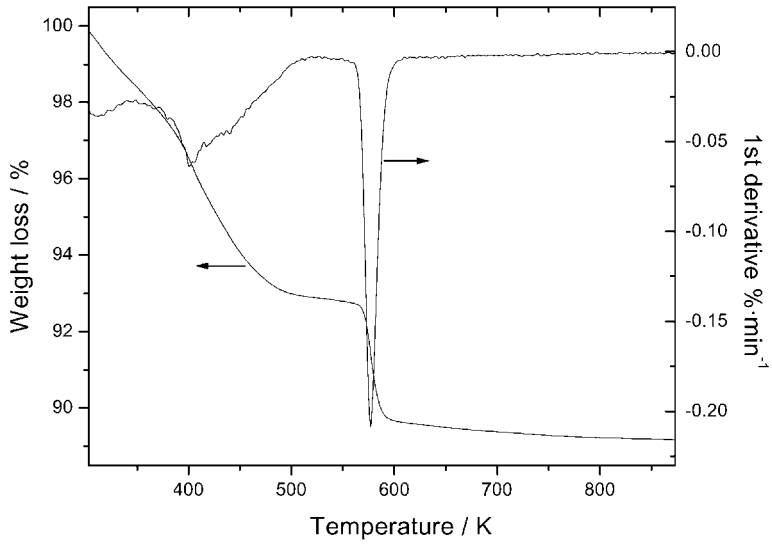

Fig. 4. TGA and DTG of sample ZnPO–CZP.

by $ZnO_3[H_2O]$ and PO_3OH groups, the "hanging" water molecule of tetrahedral Zn is lost at temperature of at least 513 K [24], although in this case no detailed assignation of the observed three-stage TG pattern is given. These results would suggest that the weight loss of the CZP phase centered at 573 K would be compatible with the existence in this compound of water linked to Zn^{2+} cations. However, unless further structure refining of this phase prove this hypothesis to be correct, the actual crystallographic data lead to the preliminary conclusion that an unusually strong water–sodium interaction takes place inside the cavities of this compound.

3.4. Thermal stability

Thermal stability of the samples has been studied by recording in situ the X-ray diffraction pattern of the materials heated in vacuum at preselected temperatures in the range 298–973 K. The results are shown in Figs. 5–7 for FAU, hopeite and CZP, respectively. In these conditions, the faujasite zincophosphate is stable up to 673 K, at 773 K a strong decrease of crystallinity is observed, and the solid recrystallizes at 873 K to a mixture of dense phases where the compound $NaZnPO_4$ [25] predominates, although the other minor individual components have not been

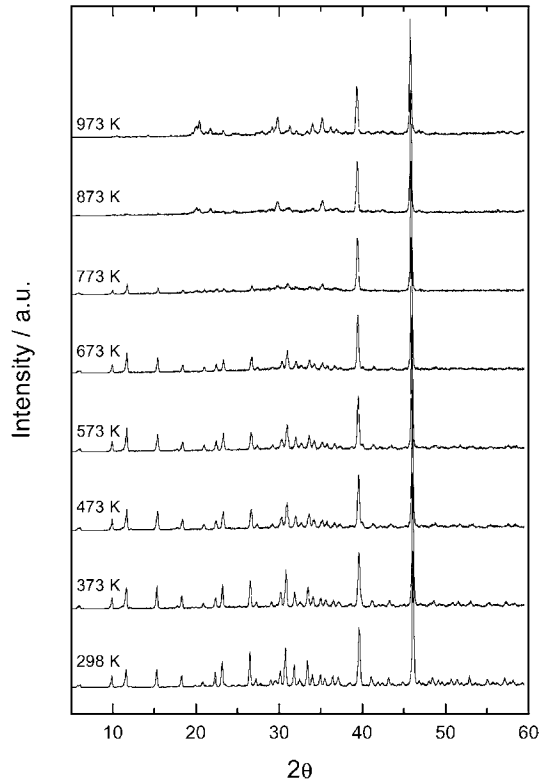

Fig. 5. In situ X-ray diffraction patterns of sample ZnPO–FAU recorded after heating the sample at different temperatures.

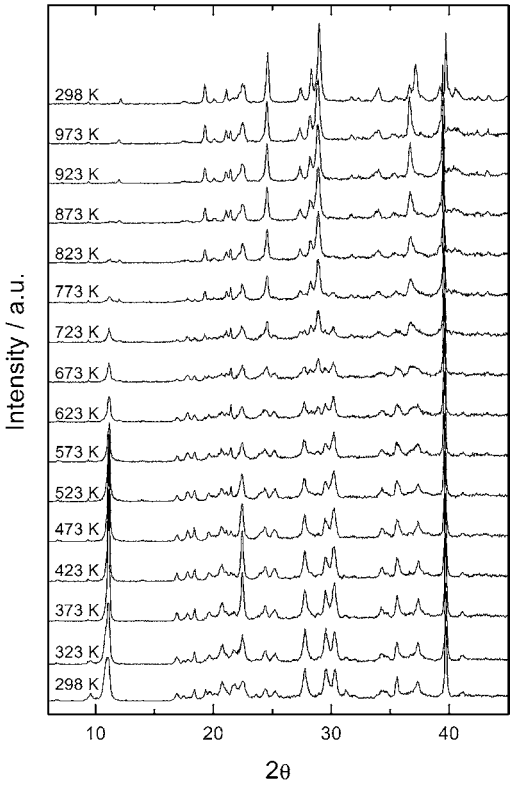

Fig. 6. In situ X-ray diffraction patterns of ZnPO–hopeite recorded after heating the sample at different temperatures and after cooling from 973 to 298 K.

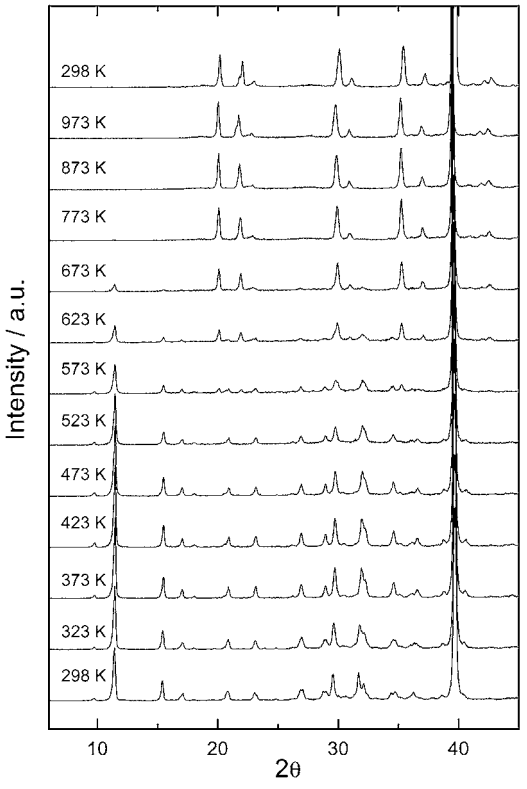

Fig. 7. In situ X-ray diffraction patterns of sample ZnPO–CZP recorded after heating the sample at different temperatures and after cooling from 973 to 298 K.

identified yet. The onset of crystallinity loss corresponds to the elimination of TMA^+ from the sodalite cages, as determined by TG (Fig. 1).

In the case of hopeite, the elimination of water molecules which were desorbed at temperatures below 500 K has little influence on the XRD pattern as shown in Fig. 6. However, the crystallinity starts to decrease if the sample is heated above ~573 K. At this temperature, some new reflections are detected, which become predominant at $T > 823$ K. These reflections correspond to a new phase identified as α-$Zn_3(PO_4)_2$ [26]. The loss of crystallinity of hopeite correlates positively with the elimination of the water molecules linked to tetrahedrally coordinated Zn^{2+} cations, which are lost in the interval 523–823 K.

The in situ XRD pattern of CZP (Fig. 7) shows a marked decrease in intensity when the sample is heated above 523 K, which is associated to the second weight loss of the TG (Fig. 4). At 773 K no hexagonal phase is detected, and the reflections present in the X-ray diffractogram can be assigned to $NaZnPO_4$ [25]. Then, the water molecules more strongly retained seems to play a key role in stabilizing the CZP structure. In the case of ZnPO–FAU, another kind of guest species, the TMA^+ cations that occupy the sodalite cages keep the structure integrity, whereas this role is play by water molecules bonded to framework Zn^{2+} cations in hopeite.

4. Conclusions

It has been demonstrated by TGA and TGA–MS that in the zincophosphate with the FAU structure synthesized in the presence of tetramethylammonium hydroxide the TMA^+ cations are incorporated into the sodalite as well as in the supercages of FAU, but the first location is preferred.

This material is stable up to 673 K and the crystallinity only decreases when the TMA^+ cations located inside the sodalite cages of the structure are eliminated (above ∼723 K)

The thermal removal of the water more strongly held by the structure in the case of CZP and hopeite produces a marked decrease of crystallinity and at higher temperatures dense zincophosphate phases are identified.

Acknowledgements

The authors acknowledge the CICYT of Spain for financial support within the Project MAT97-1207. L.A. García-Serrano acknowledges the AECI and the Instituto de Catálisis y Petroleoquímica Ph.D. Grants. The help of Dr. T. Blasco in collecting and discussing the NMR results is gratefully acknowledged.

References

[1] W.T.A. Harrison, M.L.F. Phillips, Chem. Commun. (1996) 2771.
[2] S. Neeraj, S. Natarajan, Chem. Mater. 12 (2000) 2753 and references therein.
[3] T.E. Gier, W.T.A. Harrison, T.M. Nenoff, G.D. Stucky, in: M.L. Ocelli, H.E. Robson (Eds.), Synthesis of Microporous Materials, Vol. 1, Molecular Sieves, Van Nostrand Reinhold, New York, 1991, p. 407.
[4] W. Liu, Y.L. Liu, Z. Shi, W.Q. Pang, J. Mater. Chem. 10 (2000) 1451.
[5] Y.L.W. Liu, L.Y. Na, G.S. Zu, F.S. Xiao, W.Q. Pang, R.R. Xu, J. Sol. State Chem. 149 (2000) 107.
[6] P. Reinert, N.Z. Logar, J. Patarin, V. Kaucic, Eur. J. Sol. State Inorg. Chem. 35 (1998) 373.
[7] P. Reinert, A. Khatyr, B. Marler, J. Patarin, Eur. J. Sol. State Inorg. Chem. 34 (1997) 1211.
[8] T.E. Gier, G.D. Stucky, Nature 349 (1991) 508.
[9] W.T.A. Harrison, T.E. Gier, K.L. Moran, J.M. Nicol, H. Eckert, G.D. Stucky, Chem. Mater. 3 (1991) 27.
[10] M.J. Castagnola, P.K. Dutta, Micropor. Mesopor. Mater. 34 (2000) 61.
[11] R. Singh, P.K. Dutta, Langmuir 16 (2000) 4148.
[12] T.M. Nenoff, W.T.A. Harrison, T.E. Gier, G.D. Stucky, J. Am. Chem. Soc. 113 (1991) 378.
[13] W.T.A. Harrison, T.E. Gier, G.D. Stucky, R.W. Broach, R.A. Bedard, Chem. Mater. 8 (1996) 145.
[14] N. Rajic, N.Z. Logar, V. Kaucic, Zeolites 15 (1995) 672.
[15] International Zeolite Association, Electronic Collection of Simulated XRD Powder Pattern for Zeolites, http://www.iza-sc.ethz/cgi-IZA-SC/collection, 1999.
[16] L.A. García-Serrano, T. Blasco, J. Pérez-Pariente, E. Sastre, Stud. Surf. Sci. Catal. 135 (2001).
[17] L.A. García-Serrano, J. Pérez-Pariente, F. Sánchez, E. Sastre, Stud. Surf. Sci. Catal. 130 (2000) 2987.
[18] N. Rajic, R. Gabrovsek, V. Kaucic, Thermochim. Acta 278 (1996) 157164.
[19] A. Whitaker, Acta Crystallogr., Sect. B: Struct. Sci. B31 (1975) 2026.
[20] L.S. Saldarriaga, C. Saldarriaga, M.E. Davis, J. Am. Chem. Soc. 109 (1987) 2687.
[21] S. Hayashi, K. Suzuki, S. Shin, K. Hayamizu, O. Yamamoto, Chem. Phys. Lett. 113 (1985) 368.
[22] W.T.A. Harrison, T.M. Nenoff, T.E. Gier, G.D. Stucky, Inorg. Chem. 32 (1993) 2437.
[23] W.T.A. Harrison, R.W. Broach, R.A. Bedard, T.E. Gier, X. Bu, G.D. Stucky, Chem. Mater. 8 (1996) 691.
[24] W.T.A. Harrison, T.E. Martin, T.E. Gier, G.D. Stucky, J. Mater. Chem. 2 (1992) 175.
[25] JCPDS International Center for Diffraction Data, Power Diffraction File 1-911, 1993.
[26] JCPDS. International Center for Diffraction Data, Power Diffraction File 29-1390, 1993.